

Microstructure and Dry Sliding Wear of Ti–50Al Alloy and Ti–47Al–3W/Ti₂AlC Composite Produced by Reactive Arc-Melting

Janakarajan Ramkumar¹, Santa Kumar Malhotra¹, Ramalingam Krishnamurthy¹, Hiroshi Mabuchi², Kei Demizu³, Atsushi Kakitsuji³, Hiroshi Tsuda², Toshiyuki Matsui² and Kenji Morii²

¹Indian Institute of Technology, Madras-600 036, India

²Department of Metallurgy and Materials Science, Graduate School of Engineering, Osaka Prefecture University, Sakai 599-8531, Japan

³Technology Research Institute of Osaka Prefecture, Izumi 594-1157, Japan

To study dry sliding wear behavior and its relation to microstructure, Ti–50Al alloys and Ti–47Al–3W alloy and its composite with varying reinforcement of Ti₂AlC were prepared by reactive arc-melting. Dispersion of fine B2 particles is obtained by the addition of tungsten to TiAl alloy, which improves both the hardness and wear resistance of the matrix. By adding carbon to Ti–47Al–3W alloy, composite can be produced having a random distribution of reacted rod-like Ti₂AlC particles and smaller Ti₂AlC precipitates with fine B2 particles in the matrix. The Ti–47Al–3W/3.5 vol%Ti₂AlC intermetallic composite features excellent wear resistance compared to 10 and 18 vol% composites, and fine dispersion of the Ti₂AlC and B2 particles in the matrix has improved the wear resistance properties.

(Received February 6, 2003; Accepted July 3, 2003)

Keywords: titanium aluminide, titanium–aluminum–tungsten alloy, particulate reinforced composite, reactive arc-melting, dry sliding wear

1. Introduction

Alloys based on the γ -TiAl ordered intermetallic phase show several properties that are potentially interesting for technological applications in the fields of gas turbines and automobile parts at elevated temperatures with the good oxidation resistance. These materials appear to have achieved satisfactory levels of fabricability and reliability. Studies have been devoted to the improvement of mechanical and oxidation-resistant properties by adding third elements such as Cr, Mn, Nb, V, Si or W.¹ However usage has been limited because of poor strength, fracture toughness both at room and elevated temperatures. As one possible approach to improve these properties, such alloys have recently been made as composite materials reinforced with ceramic particles like carbide, boride, nitride, and oxide.^{2–5} In addition, the introduction of ceramic particles improves wear resistance. For the TiAl exhaust engine valves, in order to protect the face and tip against the wear, the surface of the valves has been modified by the plasma carburization.⁶ This potential application is, however, still limited by the higher production cost. So main efforts of this research are to produce cost-effective TiAl composites with better wear resistance.

Traditionally, composite materials have been produced by powder metallurgy and casting technologies. In recent years, combustion reaction synthesis or self-propagating high-temperature synthesis (SHS) using powder mixture compacts has been developed to produce intermetallics or ceramics.⁷ It is also possible to form an intermetallic matrix composite with full density having ceramic dispersions using the reactive arc-melting technique.^{8,9} In the present work, Ti–50Al alloys and Ti–47Al–3W/Ti₂AlC intermetallic composites were produced using this technique. The reinforcement Ti₂AlC particles is accomplished by means of a combustion reaction. In addition, during homogenization of the carbon dissolved in the α_2 -Ti₃Al phase, precipitated Ti₂AlC particles are formed.¹⁰ Adding tungsten to the matrix has been found significantly to improve the oxidation resistance,¹¹ It

also acts as a solid solution strengthener by lowering the stacking fault energy and reduces diffusion rates so as to stabilize the $(\gamma + \alpha_2)$ lamellar structure.¹² Due to the β stabilization effect of tungsten, the Ti₂AlW(B2) phase is always formed. Tungsten can also improve the creep resistance through the precipitation of B2 particles at the lamellar interfaces,^{12–14} and the precipitation of B2 should result in better wear resistance.

Intermetallic composites thus fabricated will exhibit different tribological behavior, which depends on the properties of the matrix and reinforced particles. Nevertheless, very few reports are available in the area of TiAl intermetallic composites and wear behavior.^{15,16} The objective of this study is to investigate the microstructure and dry sliding wear behavior of Ti–50Al alloys, Ti–47Al–3W alloy and intermetallic composites with varying volume fraction of Ti₂AlC reinforcement.

2. Experimental Procedure

A reactive arc-melting technique as reported elsewhere^{9,17,18} was used to fabricate the Ti–50Al alloys and Ti–47Al–3W/Ti₂AlC composites. The powders prepared are high purity elemental powders of titanium (99.5%, –350 mesh), aluminum (99.9%, –150 mesh), tungsten (99.95%, particle size; $\sim 1\mu\text{m}$), and carbon (graphite, 99.99%, –400 mesh). The compositions of powder mixture and estimated alloy matrix, and the calculated volume fraction of reinforcement Ti₂AlC are given in Table 1. Powder mixture approximately 35 g in total was fabricated into an ingot by means of non-consumable electrode arc melting under an argon atmosphere. The arc-melted ingots were annealed at 1273 K for 144 h in a vacuum ($\sim 10^{-4}$ Pa) to assure the homogeneity of chemical composition and phase equilibrium. The phase and microstructure of samples were characterized using X-ray diffraction (XRD), optical microscope, scanning and transmission electron microscopy (SEM and TEM) and electron microprobe analysis (EPMA). Hardness

Table 1 Powder composition of the samples prepared, and estimated matrix composition, calculated volume fraction of reinforcement Ti_2AlC , and sample condition.

Sample	Powder mixture (at%)	Matrix (mol%)	Reinforcement (vol%)	Sample condition
A	Ti-50Al	Ti-50Al	—	As cast
B	Ti-50Al	Ti-50Al	—	Annealed
C	Ti-47Al-3W	Ti-47Al-3W	0	Annealed
D	Ti-46.1Al-2.9W-1.0C	Ti-47Al-3W	3.5	Annealed
E	Ti-44.5Al-2.7W-2.8C	Ti-47Al-3W	10	Annealed
F	Ti-42.5Al-2.4W-5.1C	Ti-47Al-3W	18	Annealed

values (Vickers microhardness number; Hv) were obtained as an average of ten measurements made on the matrix of each sample using a 50 g load.

Friction experiments were carried out in the laboratory at room temperature using a ball-on-flat type dry sliding wear tester as shown in Fig. 1.¹⁹⁾ The steel ball (alloy composition; 0.95%C, 1.5%Si, 0.6%Mn, 1.4%Cr, hardness; 800 Hv) was slid in reciprocating motion against the flat sample in dry condition to measure the friction coefficient and wear volume. A load of 0.93 N was applied by placing a dead weight on top of the ball specimen holder. The friction force was sensed by strain gauges, which were cemented on parallel leaf springs, and was sampled by a personal computer through an analog-digital converter. Sliding speed, sliding stroke length and sliding distance were 10 mm/min, 5 mm and 36000 mm (7200 reciprocations), respectively.

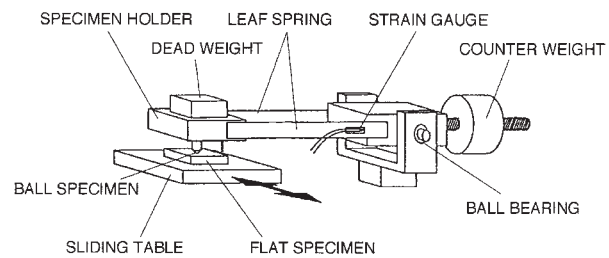


Fig. 1 Schematic drawing of pin-on-flat-type dry sliding wear tester.

This investigation used dry (unlubricated) sliding because further applications may involve temperature regimes in which many conventional lubricants would lose their effectiveness. The samples were cleaned with acetone in an ultrasonic cleaner. Separate values of the wear depths of the specimens were evaluated by means of line profiles recorded perpendicularly to the wear scars using a stylus profilometer. Measurements of the cross sectional area of the wear track were conducted at five different places and were then averaged. Wear scars and debris were characterized by means of SEM and EPMA.

3. Results and Discussion

3.1 Microstructure

Figure 2 shows the optical microstructure of the Ti-50Al alloys, the Ti-47Al-3W alloy and composites with reinforcement of Ti_2AlC . Figure 3 shows the corresponding XRD

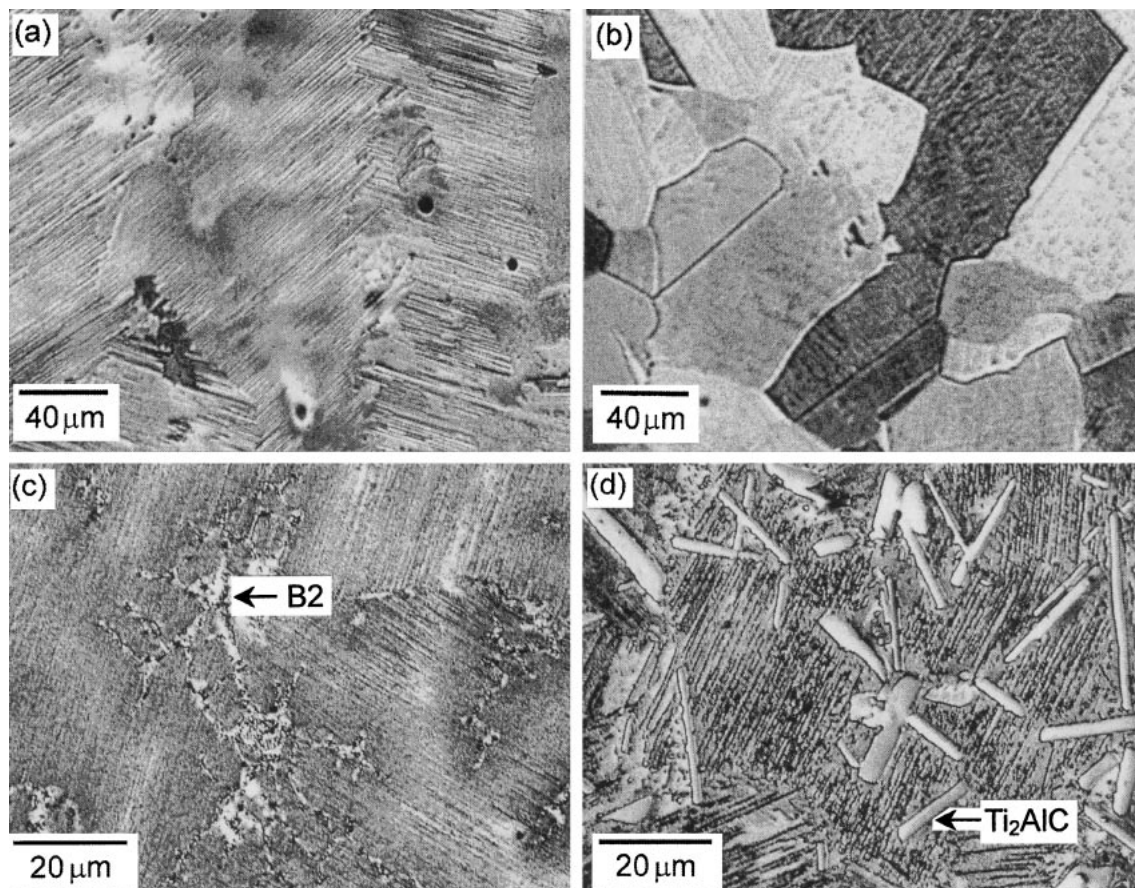


Fig. 2 Optical micrographs of (a) Ti-50Al as-cast, (b) Ti-50Al annealed, (c) Ti-47Al-3W annealed and (d) Ti-47Al-3W/18 vol% Ti_2AlC composite (annealed).

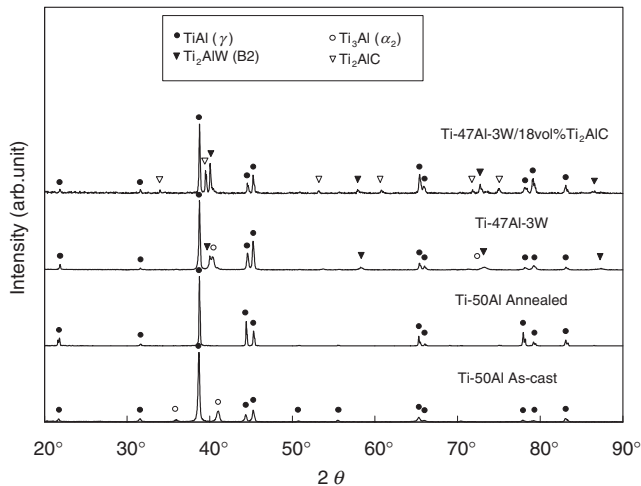


Fig. 3 XRD patterns of the samples for Ti-50 alloys, Ti-47Al-3W alloy and Ti-47Al-3W/Ti₂AlC composite.

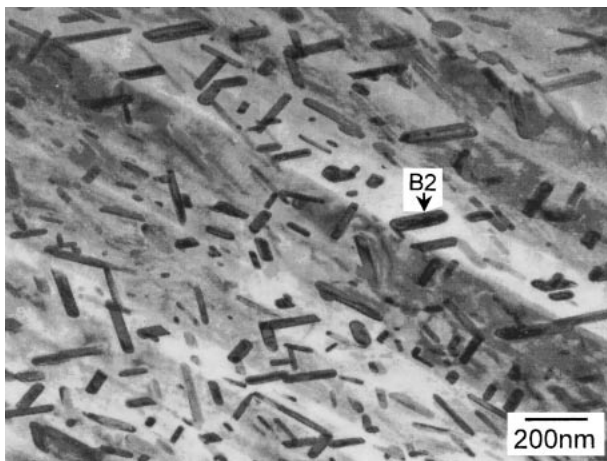


Fig. 4 TEM image of B2 precipitates in the γ matrix with traces of α_2 phase (sample: Ti-47Al-3W alloy).

patterns for the samples. The γ -TiAl, α_2 -Ti₃Al, Ti₂AlW(B2) and Ti₂AlC peaks are detected. In all the samples, no raw material peaks were observed in any of the samples. This indicates the proper reaction of the elements. In the as-cast Ti-50Al alloy, there are two phases: γ -TiAl and α_2 -Ti₃Al having a nearly lamellar structure as shown in Fig. 2(a). The above ($\gamma + \alpha_2$) two phases become a γ single phase upon annealing, as shown in Fig. 2(b). Due to the β stabilization effect of tungsten, the principal phases in the Ti-47Al-3W alloy were γ -TiAl and B2 with a small amount of α_2 -Ti₃Al (see Fig. 3). The addition of tungsten in the TiAl alloy helps in retaining the α_2 phase upon annealing.¹² Figure 2(c) shows microstructures of annealed Ti-47Al-3W alloy. The small particles around the grain boundaries were the B2 phase. In the grain, lamellar-like structure is observed. Figure 4 shows the TEM images of the lamellar-like region, and the microstructure shows the very fine B2 precipitates in the γ matrix with traces of α_2 phase. Thus the ($\gamma + \alpha_2$) lamellar grains in the matrix of as cast alloy were nearly decomposed to a γ matrix with very fine precipitates of B2 particles upon annealing.

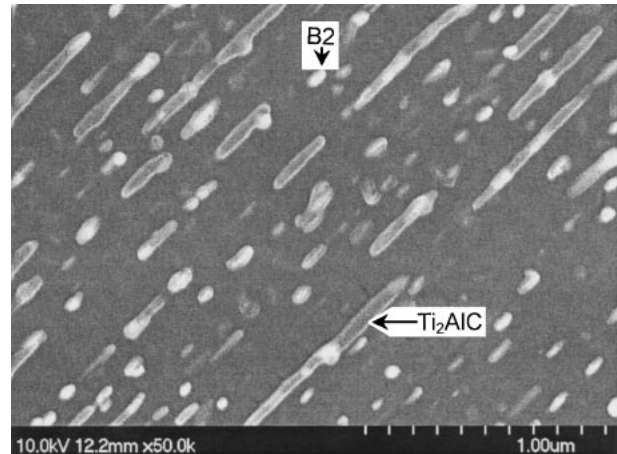


Fig. 5 SEM microstructure of the matrix for Ti-47Al-3W/18 vol%Ti₂AlC composite, showing small rod-like Ti₂AlC particles (gray contrast) and very fine B2 particles (white contrast).

For the Ti-47Al-3W intermetallic composites with 18 vol% reinforcement of Ti₂AlC, this sample has three phases: γ -TiAl, B2 and Ti₂AlC (see Fig. 3). The carbon content in the composites helps in fully decomposing α_2 -Ti₃Al upon annealing when in comparison Ti-47Al-3W alloy without carbon. As shown in Fig. 2(d), reinforcement Ti₂AlC particles are randomly distributed in the matrix. The shape is rod-like with sizes of 10–40 μ m in length, and with an aspect ratio of about 5–20 for these reinforcement particles. Smaller particles are visible in the matrix grains and appear to form in place of the decomposing lamellar structure. This microstructure was also confirmed by examination of the SEM. Figure 5 clearly shows small rod-like Ti₂AlC particles (gray contrast) and very fine B2 particles (white contrast) dispersed along the decomposed lamellar structure. The precipitation of Ti₂AlC suggests that during the annealing process the α_2 phase containing carbon is decomposed to γ -TiAl and Ti₂AlC as previously described.¹⁰ There was no change in the microstructure of the matrix with varying carbon content. On the other hand, the amount of reacted large rod-like Ti₂AlC particles clearly decreased with lower amounts of carbon content.

Table 2 shows the variation of matrix hardness among Ti-50Al alloys, Ti-47Al-3W alloy and Ti-47Al-3W/Ti₂AlC composites. The hardness for the reinforcement phase of Ti₂AlC is also shown.²⁰ With the addition of tungsten to the TiAl matrix, there is roughly a two-fold increase the hardness of the Ti-47Al-3W alloy. Dispersion of very fine B2 particles within the grain influences for increase in hardness

Table 2 Hardness of the samples, and reinforcement Ti₂AlC.

Sample	Hardness (Hv)
Ti-50Al as cast	230
Ti-50Al annealed	185
Ti-47Al-3W	480
Ti-47Al-3W/3.5 vol%Ti ₂ AlC	540
Ti-47Al-3W/10 vol%Ti ₂ AlC	595
Ti-47Al-3W/18 vol%Ti ₂ AlC	625
Ti ₂ AlC	750

of the matrix. Ti-47Al-3W/Ti₂AlC composites further increase the hardness when compared to the Ti-47Al-3W alloy. With the addition of carbon, these composites are reinforced by two types of the precipitate in the matrix: small precipitates of Ti₂AlC and very fine B2 particles (see Fig. 5).

3.2 Dry sliding wear

Friction coefficients for the flat samples slid against a steel ball increase with hardness as shown in Fig. 6. Ti-47Al-3W with 18 vol% reinforcement of Ti₂AlC had the highest friction coefficient and the lowest was reported for the annealed Ti-50Al alloy. Among the intermetallic composites, plowing action of the hard, entrapped large Ti₂AlC particles between the sliding surfaces increases the friction coefficient.

Response of wear volume for the samples sliding against a steel ball is shown in Fig. 7. The as-cast Ti-50Al alloy has better wear resistance when compared to the annealed Ti-50Al sample, and this is due to the presence of the ($\gamma + \alpha_2$) lamellar structure. The Ti-47Al-3W alloy exhibits better wear resistance than Ti-50Al alloys because of the fine dispersion of B2 particles. The Ti-47Al-3W/3.5 vol%Ti₂AlC composite has very high wear resistance when compared with all other samples. The precipitation of both small Ti₂AlC and fine B2 particles reduces the abrasive wear phenomenon and gives better wear resistance. However, a large amount of wear volume is seen on the harder composite samples with 10 and 18 vol% Ti₂AlC, where there are greater

numbers of reacted large rod-like Ti₂AlC particles along with precipitates of small Ti₂AlC and fine B2 in the matrix.

Figure 8 shows the SEM microstructures of the worn surfaces of the samples. In the samples with lower amounts of carbon content, no grooves and/or scratches are visible along the wear track, as shown in Fig. 8(a). On the other hand, in the samples with higher amounts of carbon content, a typical wear track is shown in Fig. 8(b) where deep scratches and grooves are prominent. Dry sliding of the steel ball against the sample causes the contact surface asperities to become plastically deformed and eventually welded together by high local pressure. Material from the steel ball gets transferred to the counter face, and transformed iron particles thus form a thin oxide layer along the wear track. The presence of the iron oxide layer was confirmed through EPMA. With further back and forth sliding action, the iron oxide layer fractures form small wear debris as can be seen in Fig. 8(b). These particles are harder than the original first bodies owing to strain hardening. Wear debris is indeed trapped between the sliding surfaces for a significant period of time. They cut the surface (microgrooves) creating chips, or can cause severe plastic deformation and subsurface damage, and also act like wedges in removing the large rod-like Ti₂AlC particles from the matrix. Ti₂AlC hard particles that are decohesive from the matrix, along with wear debris, act as abrasive media leading to further increase in wear volume.

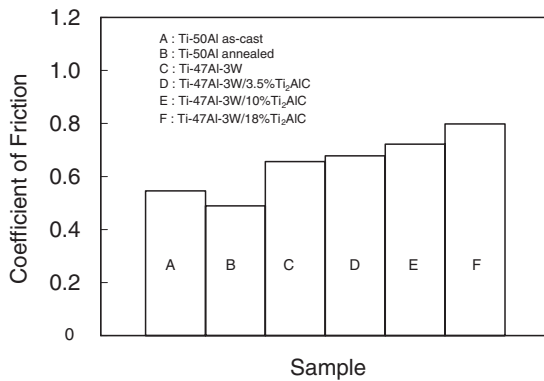


Fig. 6 Friction coefficients for the flat sample slid against a steel ball.

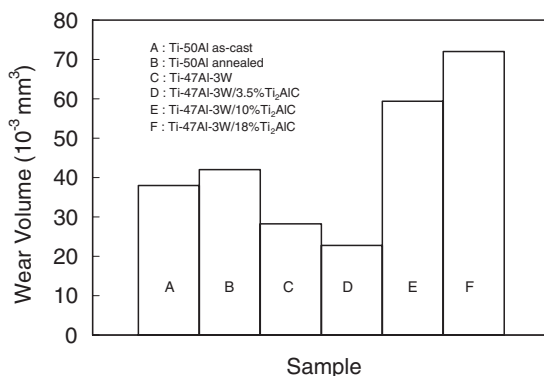


Fig. 7 Wear volumes of the samples slid against a steel ball.

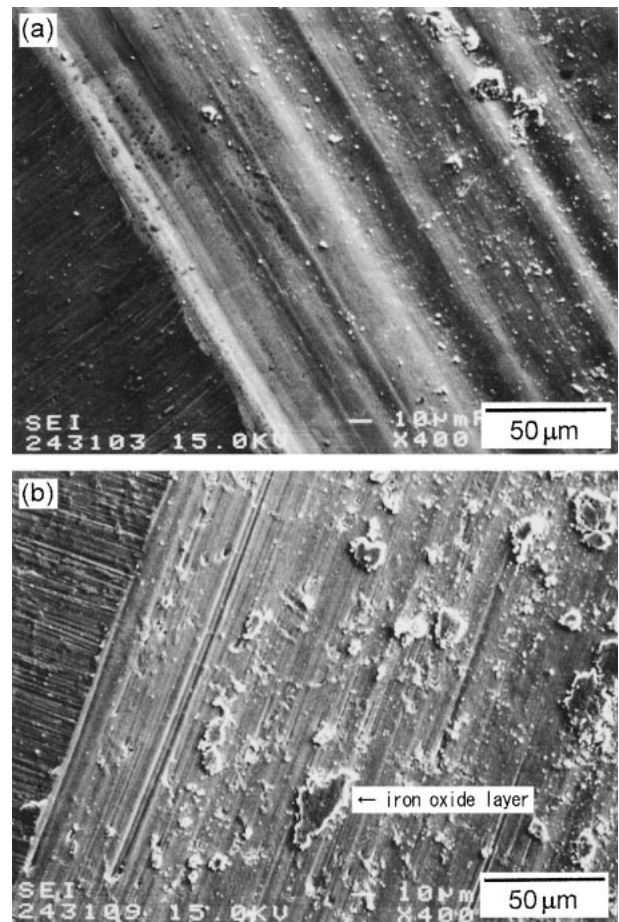


Fig. 8 SEM micrographs of the worn surfaces of the samples: (a) Ti-47Al-3W/3.5 vol%Ti₂AlC composite, and (b) Ti-47Al-3W/10 vol%Ti₂AlC composite.

4. Conclusions

(1) With the addition of tungsten to TiAl alloy, dispersion of fine B2 particles is obtained which increases the hardness and wear resistance of the matrix.

(2) With the addition of carbon to Ti-47Al-3W alloy, composites with randomly distributed large rod-like Ti₂AlC particles are fabricated, and during the annealing treatment the carbon dissolved in the matrix forms precipitated small Ti₂AlC particles. Thus Ti-47Al-3W/Ti₂AlC composites further increase the hardness by two types of the precipitate in the matrix: small Ti₂AlC and fine B2 particles.

(3) The Ti-47Al-3W/3.5 vol% Ti₂AlC composite materials revealed better wear resistance than those of Ti-50Al alloys and Ti-47Al-3W composites with 10 and 18 vol% Ti₂AlC. The improvement is attributed to the precipitation of small Ti₂AlC and fine B2 particles in the matrix.

(4) During sliding, plowing by hard large Ti₂AlC particles and wear debris play a predominant role in increasing the coefficient of friction. The abrasive interaction between the steel ball pressed against the composites with a higher volume fraction of reacted large Ti₂AlC particles causes an increase in the wear volume.

Acknowledgments

This work was supported by a Grant in Aid for Scientific Research from the Ministry of Education, Science, Sports and Culture, Japan. The authors would also like to thank the Research Institute for Advanced Science and Technology, Osaka Prefecture University.

REFERENCES

- 1) S. C. Huang: *Structural Intermetallics*, ed. By R. Darolia, J. J. Lewandowski, C. T. Liu, P. L. Martin, D. B. Miracle and M. V. Nathal (TMS, 1993) pp. 299–307.
- 2) J. C. Rawers, W. R. Wrzesinski, E. K. Roub and R. R. Brown: *Mater. Sci. Technol.* **6** (1990) 187–191.
- 3) P. S. Pao, A. Pattnaki, S. J. Cill, D. J. Michel, C. R. Feng and C. R. Crowe: *Scr. Metall. Mater.* **24** (1990) 1895–1900.
- 4) H. Mabuchi, H. Tsuda, E. Sukedai and Y. Nakayama: *J. Mater. Res.* **7** (1992) 894–900.
- 5) D. S. Shin and R. A. Amato: *Scr. Metall. Mater.* **24** (1990) 2053–2058.
- 6) S. Isobe and T. Noda: *Structural Intermetallics*, ed By M. V. Nathal *et al.*, (TMS 1997) p. 427–428.
- 7) D. Lewis: *Metal matrix composites; processing and interfaces*, ed. By R. K. Everett and R. J. Arsenault, (San Diego, CA: Academic Press 1991) p. 121.
- 8) H. Mabuchi, H. Morimoto, A. Kakitsuji, H. Tsuda, T. Matsui and K. Morii: *Scr. Mater.* **44** (2001) 2503–2508.
- 9) A. Kakitsuji, J. Ramkumar, J. Kinose, H. Mabuchi, H. Tsuda and K. Morii: *Mater. Trans.* **43** (2002) 447–450.
- 10) R. Ramaseshan, A. Kakitsuji, S. K. Seshadri, N. G. Nair, H. Mabuchi, H. Tsuda, T. Matsui and K. Morii: *Intermetallics* **7** (1999) 571–577.
- 11) D. W. McKee and S. C. Huang: *Corros. Sci.* **33** (1992) 1899.
- 12) R. Yu, L. L. He, Z. Y. Cheng, J. Zhu and H. Q. Ye: *Intermetallics* **10** (2002) 661–665.
- 13) P. L. Martin, M. G. Mendiratta and H. A. Lipsitt: *Metall. Trans. A* **14A** (1983) 2170–2174.
- 14) R. Yu, L. L. He, H. Q. Ye and J. T. Guo: *Phill. Mag. Letters* **81** (2001) 71–76.
- 15) B. Mei, J. Lin, Y. Miyamoto and M. Iwase: *ISIJ Int.* **40** (2000) 77–81.
- 16) D. E. Alman, J. A. Hawk, J. H. Tylczak, C. P. Dogan and R. D. Wilson: *Wear* **251** (2001) 875–884.
- 17) H. Nagayama, R. Ramaseshan, H. Mabuchi, H. Tsuda, T. Matsui and K. Morii: *Mater. Trans.* **41** (2000) 1064–1067.
- 18) D. Morikawa, J. Ramkumar, H. Mabuchi, H. Tsuda, T. Matsui and K. Morii: *Mater. Trans.* **43** (2002) 2193–2196.
- 19) K. Demizu, H. Ishigaki, H. Kakutani and F. Kobayashi: *J. Trib-Trans. ASME* **114** (1992) 653–658.
- 20) H. Yanagisawa, H. Tsuda, H. Mabuchi and K. Morii: *J. JNP Soc. Powder & Powder Metall.* **43** (1996) 316–320.